Calcium signals natural transformation in *Acinetobacter baumannii*

Jason Baby Chirakadavil[1]*, Kelly Goldlust[1]*, Ludovic Poiré[1], Nicolas Gaudin[1], Alexandre Chassard[1], Adrien Camilli[1,2], Manon Bouvier[1], Maria-Halima Laaberki[1,2#@], Xavier Charpentier[1#@]

1. CIRI, Center for Integrative Research in Infectious diseases and Immunology, Inserm, U1111, Université Claude Bernard Lyon 1, CNRS, UMR5308, École Normale Supérieure de Lyon, Univ Lyon, 69007, Lyon, France
2. Université de Lyon, VetAgro Sup, 69280 Marcy l'Etoile, France.

* These authors contributed equally
# Co-senior authors
@ Correspondence to Maria-Halima Laaberki, maria-halima.laaberki@vetagro-sup.fr
@ Correspondence to Xavier Charpentier, xavier.charpentier@univ-lyon1.fr

Running Head: Calcium signals natural transformation

Name	email	ORCID
Jason Baby Chirakadavil	jason.chirakadavil@gmail.com	0000-0001-8596-018X
Kelly Goldlust	kelly.goldlust@inserm.fr	0000-0003-4372-6840
Ludovic Poiré	ludovic.poire@univ-lyon1.fr	0009-0008-7763-389X
Alexandre Chassard	alexandre.chassard8@gmail.com	
Adrien Camilli	adrien.camilli@hotmail.fr	
Manon Bouvier	manon.bouvier@univ-lyon1.fr	
Maria-Halima Laaberki	maria-halima.laaberki@vetagro-sup.fr	0000-0001-5796-5995
Xavier Charpentier	xavier.charpentier@univ-lyon1.fr	0000-0001-9039-8021

Abstract

The acquisition of resistance to antibiotics in the opportunistic pathogen *Acinetobacter baumannii* may be linked to its capacity to undergo natural transformation. This mode of horizontal gene transfer relies on the import of extracellular DNA and its chromosomal integration by homologous recombination. Type IV pilus activity initiates the capture of extracellular DNA, which is then transported to the cytoplasm for recombination in the chromosome. While most *Acinetobacter baumannii* strains are transformable, the conditions allowing the expression of type IV pilus and other transformation genes remain largely unexplored. By investigating transformation-permissive conditions, we uncovered that calcium is a potent inducer of natural transformation. Type IV pilus genes and other transformation-specific genes (*comEA*, *dprA*) are upregulated by submillimolar concentrations of calcium ions, in a growth phase-dependent manner. In contrast, sodium chloride represses expression of *pilA*, counteracting the calcium-dependent induction, explaining the reported absence of transformation in NaCl-containing medium (such as LB). Independently of transcriptional induction, calcium ions also directly bind the type IV

pilus through the calcium-dependent adhesin PilY1. Our data support a model in which calcium strengthens the interaction of PilY1 with the minor pilin complex, increasing pilus dynamics and subsequent pilus-dependent DNA capture. Hence, calcium signals natural transformation through both transcriptional and structural activation of type IV pilus. In addition to providing new insights into the regulation of natural transformation in *A. baumannii* this work led us to establish a protocol for genetic engineering of *A. baumannii* by natural transformation.

Importance

Acinetobacter baumannii is a nosocomial pathogen considered a critical research priority due to its resistance to last resort antibiotics. Understanding how *A. baumannii* evolves and acquires resistance to antibiotics is thus of prime importance. This species is capable of natural transformation, a means to acquire and spread genetic information, including antibiotic resistance genes. However, the conditions under which this process is active in this species remain elusive. We identify calcium ions as potent inducers of natural transformation and propose a model of the signaling of natural transformation by calcium ions. This opens the way for further investigations into the contribution of natural transformation to acquisition of antibiotic resistance. In addition, it provides an efficient way to genetically manipulate most *A. baumannii* strains.

45 # Introduction

46 Natural transformation is one of the main mechanisms of horizontal gene transfer driving
47 the evolution of bacterial genomes (1). Over 80 bacterial species have been
48 experimentally demonstrated to be capable of natural transformation (2). This ever-
49 growing list includes *Acinetobacter baumannii*, a critical priority for research and
50 development of new therapeutic strategies (3) due to its resistance to last resort
51 antibiotics. Natural transformation likely plays a major role in the evolution of *A. baumannii*
52 genomes, constituting a route of gene exchange promoting recombination events and
53 acquisition of antibiotic resistance (4–6). Although natural transformation in *A. baumannii*
54 appears to play a limited role in overall gene acquisition, at least 15% of antibiotic
55 resistance genes had been acquired through this route (5). Indeed, even large genetic
56 elements, such as AbaR resistance islands, could be acquired by natural transformation
57 during the co-culture of *A. baumannii* isolates (7). Yet, it is the subsequent partial inhibition
58 of natural transformation by these resistance islands that favors the prevalence of
59 antibiotic resistance genes (8). Most *A. baumannii* are naturally transformable, but at
60 varying levels (9–12). Such variations in natural transformation could be ascribed to
61 genomic elements like restriction-modification systems that can limit transformation (11)
62 and prophages inhibiting transformability (10). It remained possible that not all strains
63 respond to the same stimuli for expression of transformation, yet little is known about the
64 extracellular conditions that impact the expression of natural transformation in *A.*
65 *baumannii*.

66 Natural transformation relies on the concerted expression of genes involved in DNA
67 capture, internalization and recombination in the chromosome. DNA capture is mediated
68 by extracellular filaments known as type IV pili (13). The Type IV pilus is a dynamic
69 nanomachine that undergoes cycles of extension and retraction energized by at least two
70 respective ATPase, PilB and PilT (14). Current models of Type IV pilus assembly propose
71 that a complex of minor pilins (PilX, PilW, FimT, FimU, PilV) primes the assembly of the
72 major pilin PilA to form a thin flexible filament (15–17). Pilus extension, capture of
73 extracellular DNA, followed by retraction, bring DNA to the cytoplasmic space where it is
74 bound by the ComEA receptor (13). Then DNA is converted into single-stranded DNA and
75 translocated to the cytoplasm through the ComEC channel (18) and rapidly protected by
76 DprA which recruits RecA for homologous recombination (19). Integration of DNA,

77 facilitated by the ComM helicase and YraN nuclease (20), followed by replication, results
78 in genetic transformation (21, 22).

79 The conditions and genetic control allowing the concerted expression of the genes
80 involved in natural transformation – often referred to as competence – vary between
81 species (2). For example, *Legionella pneumophila* becomes transiently competent for
82 natural transformation in the early stationary phase when the post-transcriptional
83 repression of transformation genes (Type IV minor pilins, comEA, comFC) by the
84 RocC/RocR chaperone sRNA-pair is relieved (23). In *Vibrio cholerae*, chitin induces a
85 transformation regulon, including type IV pilus genes, under control of the transcriptional
86 activator TfoX (24). In the cyanobacterium *Synechococcus elongatus*, natural
87 transformation is strictly regulated by circadian clock with Type IV pilus machinery
88 produced in the morning, and natural transformation occurring at the beginning of the dark
89 phase (evening phase) when the other genes required for transformation (including *dprA*)
90 are expressed (25). In *Acinetobacter baumannii*, the inducing signals are undefined.
91 Transformation protocols typically involve growth on agar or agarose-based solid medium
92 compatible with Type IV pilus-mediated motility (7, 9, 26–30). Although the signals
93 remained elusive, natural transformation was found to occur at the beginning of the growth
94 phase and linked to the expression of type IV pilus genes (28).

95 Here, we explored the regulation of natural transformation in *Acinetobacter baumannii* by
96 experimental conditions. Using a selection-free luminescence-based assay for natural
97 transformation we screened a wide range of conditions, ultimately identifying a trigger of
98 natural transformation. Genetics and molecular modeling indicate that calcium ions induce
99 transformation by both signaling expression of the Type IV pilus and stabilization of the
100 pilus assembly. The identified conditions allow the natural transformation of *A. baumannii*
101 with high efficiency in liquid medium, opening the way for further investigations into the
102 dynamics of transformation but also facilitating genetic engineering of this opportunistic
103 pathogen.

104 Results

105 Mechanical sensing is not involved in induction of natural transformation

106 Natural transformation of *A. baumannii* is routinely done on medium solidified with agar or
107 agarose (7, 9, 26–30). However, we and others have experienced inconsistent results that
108 could be linked to the source of the agar or agarose used to solidify the medium. To
109 formally establish this, we tested five references of agarose powders from four suppliers.

110 Used at the same concentration (15 g/L) all agarose powders have identical solidifying
111 power. We tested natural transformation of strain AB5075 using the NanoLuc (Nluc)
112 transformation assay previously reported (10). Briefly, a suspension of AB5075 is spotted
113 on the agarose plated together with a plasmid DNA that cannot replicate in *A. baumannii*
114 but that carries the *nluc* gene flanked by 2 kb-long regions homologous to the
115 chromosome. Import and recombination of this sequence leads to expression of Nluc in
116 the transformants which can be detected by measuring luminescence with the Nluc
117 substrate furimazine. We previously established that the luminescence signal is linearly
118 correlated with the number of transformants over eight orders of magnitude (R^2=0.99).
119 Using this assay we found that only two of the tested agarose could generate
120 transformants with RFU up to 10^6 (Fig. 1A), corresponding to transformation frequencies of
121 10^{-3}-10^{-4}. Three other agarose gave luminescence signal barely above the value of the
122 control without DNA ($2x10^2$ RFU). This suggested that either the perception of a solid
123 surface is required to induce transformation but some agarose contain an inhibitor, or the
124 perception of a solid surface is dispensable for induction but some agarose contain an
125 inducer of transformation. We tested this latter hypothesis by extracting any water-soluble
126 compound from the unmelt agarose powder of the Euromedex D3 agarose that is
127 permissive for transformation. A D3 agarose soluble extract (ASE) in liquid tryptone
128 medium strongly induces transformation of strain AB5075, up to 10^7 RLU (transformation
129 frequency of 10^{-2}), a 10,000-fold increase relative to a no-agarose liquid tryptone medium
130 (Fig. 1B). As expected, no transformation was observed in an AB5075 *comEC* mutant.
131 This shows that the D3 ASE contains a water-soluble potent inducer of natural
132 transformation, aguing against a mechanical triggering of natural transformation.

133 **A soluble molecule induces a growth phase-dependent regulon of natural**
134 **transformation**

135 Natural transformation in *A. baumannii* was previously found regulated by the growth
136 phase, correlating with the expression of Type IV pilus genes (28). To determine how the
137 ASE stimulates transformation, we tested the transformability of bacteria over the growth
138 curve. We confirmed previous results, showing that transformation peaks at 3 hours post-
139 inoculation, corresponding to the exponential growth phase (Fig. 1C). Transformation
140 stimulated by ASE followed the same kinetic, peaking at 3 hours, with a wider
141 transformation window but also falling under the detection limit in the stationary phase at 7
142 hours post-inoculation (Fig. 1C). We then tested if increased transformation was tied to
143 type IV pilus induction. To do so, we compared the effect of ASE from inducing (D3) and

non-inducing agarose (Roth) on the global transcriptome using RNAseq profiling at 3 hours post-inoculation. Each of the non-inducing (Roth) (Fig. 2D) and inducing (D3) agarose (Fig. 2E) downregulate specific set of genes (blue dots). Yet, they also downregulate the expression of the same genes (green dots) including the phenylacetic acid catabolic pathway (*paaA*, *paaB*, *paaC*, *paaX*, *paaK*, *paaZ*). This clearly shows that adding agarose to culture medium is not without consequences on gene expression. Most importantly, while the Roth ASE induces only a dozen genes, the D3 ASE induces the upregulation of nearly all type IV pilus genes, several of which are organized in operons (*pilMONPQ*, *pilA*, *fimU-pilVWXY1-pilE1-pilE2*, *pilGHIL-chpA*, *pilBCD*), but also transformation-specific genes such as *yraN*, *dprA* or *comEA* (Fig. 1E and Fig. 1F). Notably, all of these genes are downregulated in the stationary phase (D3 ASE, 7 hours) relative to the exponential phase (D3 ASE, 3 hours) (Fig. 1F). Hence, a water-soluble compound present in agarose preparations induces a growth-phase regulated transformation regulon.

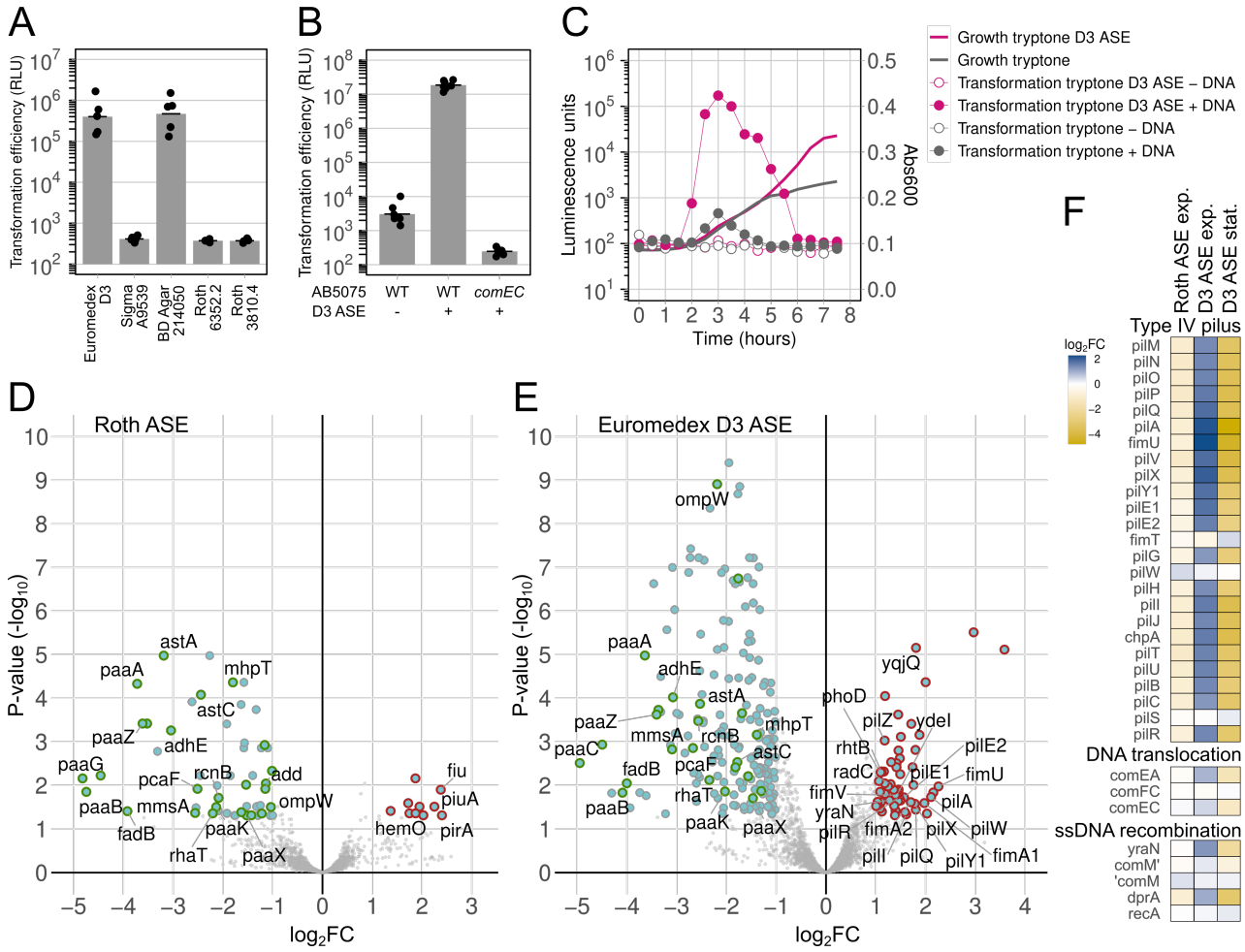

Figure 1. A water-soluble molecule induces a growth phase-dependent regulon of natural transformation.
A. Efficiencies of natural transformation of *A. baumannii* strain AB5075 in tryptone medium solidified by different agaroses. Transformation is determined by incubating with a DNA fragment containing the Nluc gene flanked by 2 kb-long sequence of homology with the chromosome on each side. Transformants are

detected by luminescence units (LU) produced when adding the substrate furimazine, and expressed relative to the optical density of the culture (RLU). The detection limit, and background luminescence is 10^2.
B. Efficiencies of natural transformation of strain AB5075 in liquid tryptone medium or tryptone agarose soluble extract (ASE) using the powder of the Euromedex D3 agarose. The method is identical as in panel A.
C. Growth and natural transformation of strain AB5075 in tryptone medium or tryptone agarose soluble extract (ASE) using the powder of the Euromedex D3 agarose. Growth of the culture is monitored by reading the absorbance at 600 nm (Abs_{600}). Transformation efficiency is tested at 30 minutes interval by addition of transforming DNA for 30 minutes followed by the addition of DNAse I. The culture is then further incubated. All samples were analyzed for luminescence signal, indicating effective transformation, at the end of the kinetic.
D and E. RNAseq analysis of strain AB5075 grown for 3 hours in tryptone and tryptone using the non-transforming Roth agarose (D) or the transforming Euromedex D3 agarose (E). In both panel D and E, differentially-expressed genes ($log_2FC<-1$ or $log_2FC>1$ and P-value<0.05) are shown in blue. Genes down-regulated in both conditions are highlighted in green. Genes specifically upregulated by each condition are highlighted in deep red.
F. Variation in expression of selected genes, required for natural transformation, in Roth ASE, D3 ASE and in D3 ASE at 8 hours (stationary phase) compared to D3 ASE at 3 hours (exponential phase). In AB5075, the *comM* gene is disrupted by the insertion of an AbaR element, forming two pseudogenes (*comM*' and '*comM*).

157 **Screen identifies Ca and Mg as inducers and NaCl as repressor**

158 RNAseq profiling revealed no upregulated genes involved in metabolism, suggesting that
159 the transformation inducer is not metabolizable. Chemical preparations are often
160 contaminated by ions and salt. We thus screened the Biolog PM-PM5 plates containing
161 four undisclosed concentrations of ions for induction of natural transformation. This
162 revealed strong induction by $CaCl_2$ and to a lesser extent by $MgCl_2$ (Fig. 2A). Addition of
163 $CaCl_2$ or $MgCl_2$ to the tryptone medium strongly stimulated natural transformation, in a
164 dose-dependent manner (Fig. 2B). $CaCl_2$ is a stronger inducer, matching the induction by
165 the D3 ASE (Fig. 2B), yet $CaCl_2$ and $MgCl_2$ showed the same dose-response effect, with
166 maximal induction at 0.68 mM, suggesting the same mechanism of action. Indeed, the
167 effects of $CaCl_2$ and $MgCl_2$ are not additive (Fig. 2C). Although $CaCl_2$ is a stronger inducer
168 than $MgCl_2$, $MgCl_2$ shows stimulation of growth like observed for D3 ASE in the stationary
169 phase (Fig. 2D and Fig. 1C). This suggested that D3 ASE contained Ca^{2+} ions stimulating
170 transformation as well as Mg^{2+} ions stimulating growth. To test this hypothesis, we
171 evaluated the effect on growth of adding the Ca^{2+}/Mg^{2+} chelator EDTA to the medium.
172 EDTA at 0.1 mM abolished growth indicating that the tryptone medium readily contains
173 trace amounts of Ca^{2+} (less than 0.1 mM, given the 1:1 stoichiometry of EDTA:cation).
174 Adding $CaCl_2$ at 0.68 mM did not change the growth yield (same final absorbance), but
175 growth is expectedly inhibited at EDTA concentration of at least 0.8 mM. D3 ASE improved
176 growth yield, identically to adding $MgCl_2$ at 0.68 mM, and for both an EDTA concentration
177 of 0.8 mM is needed to prevent growth. Thus, given the increased growth of D3 ASE and
178 its effect on transformation similar to that of adding $CaCl_2$, we conclude that D3 ASE

179 contains both Ca^{2+} and Mg^{2+} ions, in undetermined concentrations, but likely greater than
180 0.68 mM.

181 Screening for the effect of ions on transformation, we also observed reduced
182 transformation with increasing amounts of NaCl (Fig. 2A). This was confirmed in tryptone
183 medium as well as when tryptone supplemented with $CaCl_2$ (Fig. 2E). NaCl at
184 concentration greater than 0.07% inhibits transformation and completely abolishes it at
185 1%, which is the typical concentration of the commonly used lysogeny broth (LB medium).
186 This is consistent with previous results obtained with strain A118 (29). In LB medium,
187 $CaCl_2$ was previously reported to only moderately induce transformation in strain A118
188 (31). In this strain, we confirmed that $CaCl_2$ has a modest effect in standard LB, and also
189 found no effect of $MgCl_2$ (Fig. 2F). The results suggest that LB might readily contain
190 enough Mg^{2+} and a sub-optimal amount of Ca^{2+} to induce transformation but that the
191 induction is counteracted by inhibition by NaCl. Consistent with this hypothesis, LB
192 prepared without NaCl (LB no salt) produces a 500-fold increase in transformation, with a
193 further increase when supplemented with $CaCl_2$, while $MgCl_2$ had no additional effect (Fig.
194 2E).

195 Having identified the optimal conditions for natural transformation, we tested these on a
196 panel of strains, including commonly used laboratory strains. Transformation medium
197 ($CaCl_2$ 0.68 mM, no NaCl) improved transformation of most strains, including CNRAB1
198 and 40288, which were non-transformable in the absence of supplementation (Fig. 2G).
199 Addition of $CaCl_2$ also further increased transformation of the highly transformable strain
200 A118, but did not change the transformation of the M2, 29D2 and 31D1 strains which
201 readily showed high transformation levels in the absence of $CaCl_2$ supplementation.

202 In conclusion, $CaCl_2$ and to a lesser extent $MgCl_2$, induce natural transformation. Both
203 divalent cations are the likely contaminants contained in the transformation-inducing
204 agarose. Adding $CaCl_2$ to a tryptone medium without sodium chloride allows *A. baumannii*
205 to undergo natural transformation in liquid medium, further demonstrating that surface
206 sensing is dispensable for this type IV pilus-mediated process.

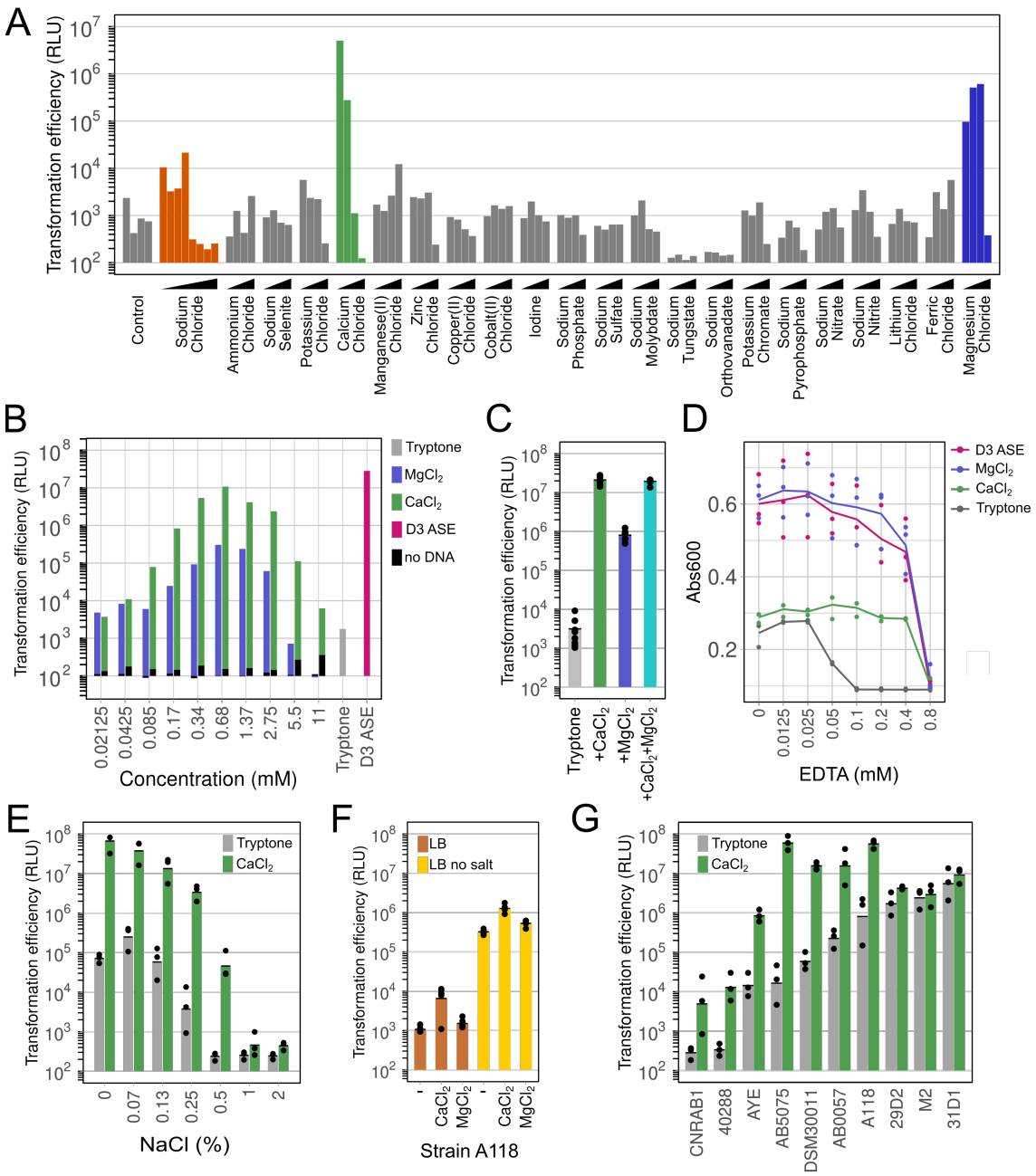

Figure 2. Induction of natural transformation by calcium and magnesium is antagonized by sodium chloride

A. Natural transformation of strain AB5075 in tryptone medium supplemented with the dried content of the Biolog PM-PM5 plate.

B. Natural transformation in tryptone medium supplemented with increasing concentration of $CaCl_2$ or $MgCl_2$.

C. Natural transformation in tryptone medium supplemented with $CaCl_2$ (0.68 mM) or $MgCl_2$ (0.68 mM) or both. Bars represent the average of technical replicates.

D. Effect on growth of EDTA on tryptone medium and D3 ASE, measured at 16 hours post-inoculation by absorbance reading at 600 nm. Data are presented as average values of three independent experiments.

E. Natural transformation in tryptone medium and tryptone supplemented with $CaCl_2$ (0.68 mM) at an increasing concentration of NaCl. Bars represent the geometric average of three independent experiments.

F. Effect of $CaCl_2$ and $MgCl_2$ on natural transformation of A118 in LB and LB no salt. Bars represent average of five technical replicates.

G. Natural transformation of a panel of *A. baumannii* and *A. nosocomialis* (M2) strains in tryptone medium alone or supplemented with $CaCl_2$ (0.68 mM). Bars represent the geometric average of three independent experiments.

207 **Ca^{2+} and Mg^{2+} are equivalent in inducing expression of transformation genes,**
208 **independently of T4P activity**

209 In order to understand the mechanism by which $CaCl_2$ and $MgCl_2$ induce transformation,
210 we analyzed the transcriptome of AB5075 exposed to $CaCl_2$ or $MgCl_2$ in the exponential
211 growth phase. Consistent with D3 ASE containing calcium/magnesium salts, $CaCl_2$ and
212 $MgCl_2$ induce the upregulation of the type IV pilus genes and other natural transformation
213 genes (*comEA*, *dprA*) (Fig. 3A). The transcriptional responses to $CaCl_2$ and $MgCl_2$ are
214 strikingly similar, indicating that the two metal ions are sensed by a common signaling
215 pathway. With the *pilA* gene being upregulated and a central component of type IV pilus
216 regulation and activity, we followed its expression using a transcriptional fusion of the full
217 *pilA* gene to *gfp* (*pilA*::*gfp*) in a Δ*pilA* mutant. In agreement with the RNAseq data, *pilA* is
218 induced to the same extent by $CaCl_2$ and $MgCl_2$ and is expressed during the exponential
219 phase and then repressed in the stationary phase (Fig. 3B). The inhibition of
220 transformation by NaCl suggested that it counteracts the Ca^{2+}-induced expression of the
221 type IV pilus. Indeed, in the presence of calcium, *pilA* expression is repressed by
222 increasing concentration of NaCl, indicating that inhibition of natural transformation is the
223 consequence of a transcriptional response to NaCl (Fig. 3C).

224 The coordinated expression of the type IV pilus and the genes required for DNA
225 import/recombination is indicative of a mechanism that equally senses Ca^{2+} and Mg^{2+} ions
226 and triggers a transcriptional response. It is not currently known how the *comEA* and *dprA*
227 genes are regulated in *A. baumannii*, but regulation of type IV pilus in *A. baumannii* has
228 some similarities with the better-known regulation in *P. aeruginosa*. The chemosensory
229 systems Pil-Chp (32), could have been a candidate sensor/regulator, yet in *A. baumannii*,
230 the absence of *chpA*, *pilG*, or *pilH* in transformation conditions (D3 agarose) did not
231 change the *pilA* transcript levels (28). Expression of the major pilin PilA is under control of
232 the two component PilRS system which can increase *pilA* transcription in response to low
233 levels of periplasmic PilA caused by its mobilization in the extended pilus (33). In addition,
234 in *P. aeruginosa* the minor pilin PilY1 was found to act as a Ca^{2+}-dependent regulator of
235 bacterial surface motility, favoring cycles of pilus extension/retraction (34). Hence, we
236 hypothesized that PilY1 could sense Ca^{2+}, activates pilus dynamics, which would in turn
237 trigger *pilA* transcriptional activation through the PilRS system. To test this hypothesis, we
238 deleted the *pilY1* gene, which, as shown for several species including *Acinetobacter baylyi*
239 should cause complete loss of pilus assembly (34–36). As expected, the Δ*pilY1* mutant is
240 completely defective for natural transformation (Fig. 3D). However, the loss of PilY1 did not
241 alter the transcriptional activation of *pilA* in response to $CaCl_2$ as determined at the

242 populational level (Fig. 3E) and at the single cell level (Fig. 3F and 3G). Thus,
243 transcriptional activation of *pilA* occurs independently of type IV pilus dynamics. In
244 conclusion, Ca^{2+} and Mg^{2+} ions alike induce a transcriptional response mainly increasing
245 the expression of type IV pilus and transformation genes. Interestingly, although $CaCl_2$ and
246 $MgCl_2$ induce transcriptional activation of the same magnitude, $CaCl_2$ can increase
247 transformation 10- to 20-times more than $MgCl_2$ (Fig. 2B and Fig. 2C), suggesting that its
248 transformation-stimulating effect is not solely due to increased pilus expression.

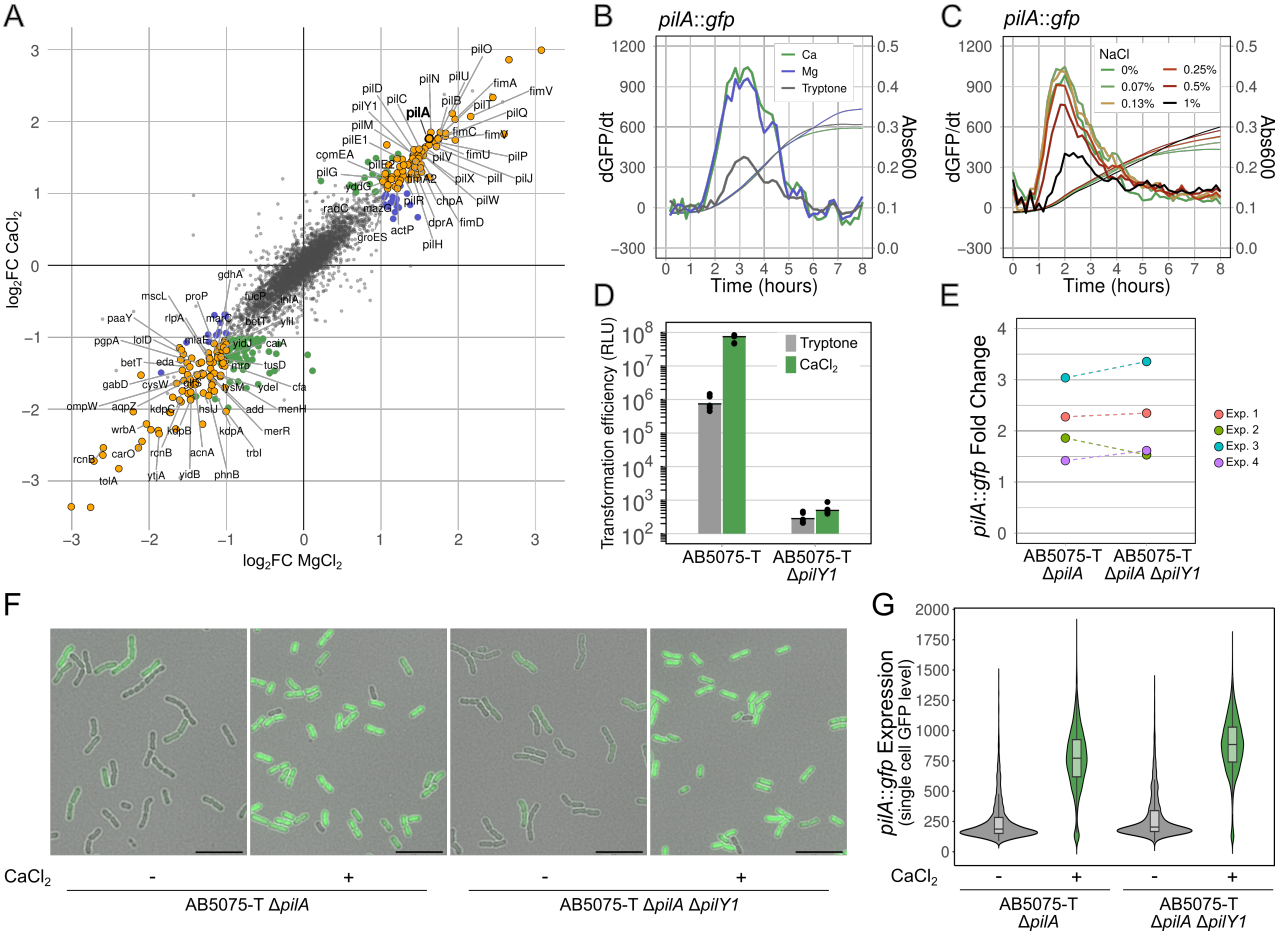

Figure 3. Calcium and magnesium induce a type IV pilus and transformation regulon.
A. RNAseq analysis of AB5075 grown for 3 hours in tryptone medium or and tryptone medium supplemented with $CaCl_2$ or $MgCl_2$. Differentially-expressed genes (log2FC<-1 or log2FC>1 and P-value<0.05) in both $CaCl_2$ and $MgCl_2$ conditions are shown in yellow. Genes specifically differentially-regulated by $CaCl_2$ and $MgCl_2$ are highlighted in green and blue, respectively.
B. Expression of a transcriptional fusion of the *pilA* gene to *gfp* in AB5075-T Δ*pilA*. Bacterial growth (Abs_{600}) and change in *pilA*::*gfp* expression relative to cell density (dGFP/dt, arbitrary units) were measured every 10 min over an 8-h period. $CaCl_2$ and $MgCl_2$ were added to tryptone medium at 0.68 mM.
C. Same as B, with increasing concentrations of $CaCl_2$ in tryptone medium.
D. The PilY1 minor pilin is essential for natural transformation in strain AB5075. Transformation conditions are identical to those of Figure 2. Presented data are an average of three independent experiments.
E. Fold-change in *pilA*::*gfp* expression caused by $CaCl_2$ at 0.68 mM in AB5057-T Δ*pilA* and AB5075-T Δ*pilA* Δ*pilY1*. Expression kinetics were recorded as in panel B, and fold-change represents the ratio of the maximal dGFP/dt of the $CaCl_2$ condition relative to tryptone alone. Individual results from four independent experiments are shown.
F. Fluorescence microscopy *pilA*::*gfp* expression in AB5057-T Δ*pilA* and AB5075-T Δ*pilA* Δ*pilY1* with or without $CaCl_2$. Scale bars (bottom right corner) represent 10µm.
G. Single cell expression of *pilA*::*gfp* expression in AB5057-T Δ*pilA* in tryptone medium with (n=4680,

median level=772) or without $CaCl_2$ (n=2449, median level=187), and AB5075-T Δ*pilA* Δ*pilY1* with (n=4373, median level=885) or without $CaCl_2$ (n=2848, median level=203). Results are from two independent experiments.

Calcium stabilizes the minor pilin complex

In *P. aeruginosa*, recent structural analyzes show that PilY1 forms a champagne cork like-structure that plugs PilQ secretin and primes the minor pilins facilitating Type IV pilus assembly and dynamics (16). Ca^{2+} binding to the conserved calcium binding loop of PilY1 is proposed to inhibit PilT-mediated pilus retraction, while in the absence of calcium pilus retraction is favored (34). We hypothesize that in *A. baumannii*, Ca^{2+} could also have a structural effect on the PilY1-minor pilin complex, directly influencing the dynamics of the pilus and, consequently, natural transformation. We first modeled PilY1 in complex with the minor pilins PilX, PilV, PilW, FimU, FimT, PilE1, PilE2 and PilA major protein using Alphafold3. Modeling of the PilY1-PilA-minor pilin complex produced a top rank model, with metrics indicating a good confidence for the overall topology (pTM of 0.72) and for inter-protein interface (ipTM of 0.73) (Fig. 4A). The modeled structure of PilY1 exhibits the characteristic architecture described in the crystal structure of PilY1 of *P. aeruginosa* (34), with an N-terminal globular head domain and a C-terminal beta-propeller fold (Fig. 4A). Importantly, the model shows that the beta-propeller fold makes direct contact with the minor pilin complex, in agreement with previously proposed pilus assembly models, based on genetic and biochemical evidence in *P. aeruginosa* (16, 37) and on cryo-electron tomography and protein interaction networks of the *M. xanthus* pilus (17). PilX is positioned directly below the C-terminal domain of PilY1 and appears to be the only direct contact with PilY1. The others minor pilin (PilV, PilW, FimT, FimU, PilE1, PilE2) and the major pilin PilA show no direct contact with PilY1 but organize into a compact helical bundle positioned beneath or beside PilX (Fig. 4A). These observations suggest that PilX may act as a structural bridge between the minor pilin complex and PilY1, potentially serving as a central element of type IV pilus initiation complex. To locate the calcium binding site on PilY1, we next modeled PilY1 in complex with PilX and performed a Ca^{2+} docking using Alphafold3. The best model exhibits a high ranking confidence of 0.8, a pTM of 0.76, an ipTM of 0.81. Two Ca^{2+}-binding motifs are predicted. One is located in the N-terminal globular head domain and has no known function, and was not present in the crystal structure of the *P. aeruginosa* PilY1 (34). The other one is located in the beta-propeller and correspond to the one required for twitching motility in *P. aeruginosa* (34) (Fig. 4B). Given that the only direct interaction of PilY1 with PilX involves the beta-propeller fold containing the calcium binding site, we next tested the role of Ca^{2+} binding to

the PilX-PilY1 interaction. To do so, we performed a molecular mechanics, generalized Born surface area calculation (MMGBSA) in presence or absence of Ca^{2+} and estimated the binding free energy (ΔG_bind) (Table1). This approach assesses how Ca^{2+} influences the stability and interaction strength between PilY1 and PilX. To ensure robustness and reproducibility, we performed two independent simulations, each on 5 structural models, including the best model presented in (Fig. 4B). In the absence of divalent cation, ΔG_bind values ranged between -195 and -210 Kcal/mol depending on the model, with negative values indicating stable interaction between PilY1 and PilX. In the presence of Ca^{2+}, ΔG_bind values ranged between -212 and -230 Kcal/mol corresponding to a ΔΔG values of -18,77 Kcal/mol compared to the condition without Ca^{2+}. This decrease of binding free energy value clearly supports that Ca^{2+} enhances the stability of PilY1-PilX complex. In contrast, in the presence of a Mg^{2+} ion, ΔG_bind values ranged between -188 and -207 Kcal/mol with a ΔΔG values of –2,34 Kcal/mol compared to the condition without ion. This small change in binding free energy indicates that the Mg^{2+} has a moderate role in stabilizing PilY1-PilX complex. To validate these results, we also performed the more computationally intensive molecular mechanics Poisson-Boltzmann surface area (MMPBSA) calculation. Consistent with the MMGBSA results, the MMPBSA analysis confirmed that Ca^{2+} binding strengthens the PilY1-PilX interaction (Table S3). To further investigate the role of this calcium binding loop in natural transformation, we introduced in PilY1 the substitution D947A predicted to impair Ca^{2+} coordination without altering the overall structure of PilY1 (Fig. 4C) (34, 38). In agreement with predictions, transformation efficiency is drastically reduced in the D947A substitution compared to the wild type (Fig. 4D). Taken together, the results indicate that Ca^{2+} helps stabilize the PilY1-PilX complex. Ca^{2+} binding, more than Mg^{2+}, strengthens the interaction between PilY1 and PilX, which in turn promotes the recruitment of the other minor pilins and favors type IV pilus assembly.

Condition	replicate	ΔG_bind (best model)	Mean ΔG_bind (5 models)	ΔΔG (best model)	ΔΔG (5 models)
No ion	N1	-212.69	-194.52		
	N2	-227.06	-209.74		
	Mean	-219.88	-202.13	0	0
Calcium	N1	-246.02	-211.53		
	N2	-221.18	-230.27		
	Mean	-233.6	-220.9	-13.72	-18.77
Magnesium	N1	-206.99	-183.13		
	N2	-237.45	-207.32		
	Mean	-222.22	-197.73	-2.34	4.4

Table 1 : Binding free energy of PilY1-PilX. Binding free energy of PilY1-PilX (ΔG_bind) in the absence (control) or presence of Ca^{2+}/Mg^{2+}. Energy was calculated using MMGBSA (CHARMM36, GB8). ΔG_bind are shown for both replicate (N1,N2) of the mean of 5 independent structural models and the best model. ΔΔG values is the binding free energy difference between the control and the others conditions. A decrease of ΔΔG reflects a higher complex stability.

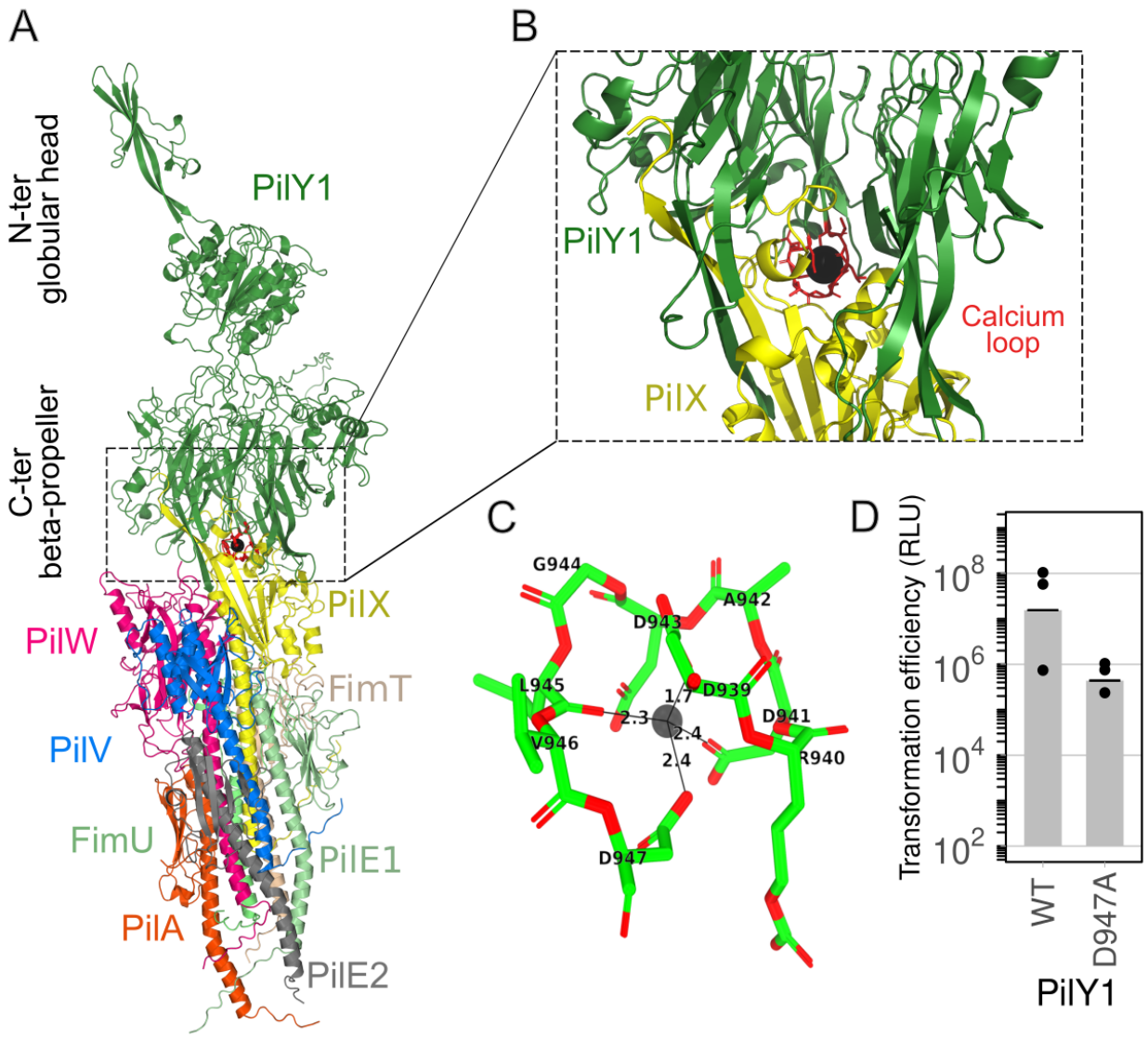

Figure 4 : Calcium stabilizes the PilY1-minor pilin complex.
A. Alphafold multimer modeling of PilY1, Type IV minor pilins and major pilin complex. Structure confidence metrics best model ipTM = 0.69, pTM = 0.71, ranking confidence = 0.73. Cartoon representation PilY1 (green), PilX (yellow), PilA (orange), PilV (blue), PilW (hotpink), FimU (lime), FimT (wheat).
B. Close up on the AlphaFold model of PilY1 and PilX with calcium docking and highlighting the calcium-binding loop (red). Structure confidence metrics ipTM = 0.80, pTM = 0.76, ranking confidence = 0.81. PilY1 (green), PilX (yellow).
C. Calcium binding loop modeling with relative distance in angstroms.
D. Natural transformation of AB5075-T encoding the wild-type PilY1 (WT) or the PilY1 D947A substitution in the presence of $CaCl_2$. Presented data are an average of three independent experiments.

311 ## Discussion

312 We here report the conditions that are permissive to natural transformation in *A. baumannii*
313 in liquid medium. Up until now, natural transformation of *A. baumannii* required the use of
314 solid medium, and DNA uptake seemed to correlate with type IV pilus-dependent motility
315 (26–28, 30). It could be hypothesized that surface sensing was the trigger for expression
316 of the Type IV genes, and possibly also for other transformation genes that are needed to

317 take up and recombine DNA. This hypothesis is supported by work in *P. aeruginosa* and
318 *Caulobacter crescentus* showing that the surface-dependent resistance to pilus retraction
319 is a trigger for intracellular signaling, further inducing Type IV pilus genes, virulence or
320 chemotaxis genes (14, 39, 40). Here we found that transformation can occur in liquid
321 medium if supplemented with submillimolar concentrations of $CaCl_2$ or $MgCl_2$. Under these
322 conditions, the bacteria are not attached to a surface and cycles of extension-retraction
323 would occur in planktonic cells, allowing the capture of extracellular DNA, likely through
324 the binding to the minor pilin PilT (41). Activation of Type IV pilus in liquid medium is also
325 supported by the $CaCl_2$-dependent and PilA-dependent formation of large planktonic
326 clumps of cells (Fig. S1). Activation of Type IV pilus, and processes that depend on it, can
327 thus be achieved in the absence of surface sensing by supplementing the medium with
328 calcium ions. Interestingly, our earlier findings suggested that $CaCl_2$ and $MgCl_2$ had
329 minimal impact on transformation (9). These experiments used transformation conditions
330 based on agarose D3, which we show here readily contains calcium and magnesium ions
331 at levels sufficient for optimal transformation efficiency, hence explaining the lack of effect
332 of additional calcium or magnesium ions. Another work also reported that $CaCl_2$ can
333 induce transformation in the *A. baumannii* strain A118 in LB medium but with only a 4-fold
334 increase in transformation frequencies, a much weaker effect than the >1,000-fold
335 increase reported here. We did confirm here the weak induction of $CaCl_2$ in LB medium,
336 and show it to be due to the presence of NaCl inhibiting transformation (Fig. 2E). Sodium
337 chloride was indeed previously reported to inhibit transformation, causing a 100-fold
338 decrease in transformation frequencies in A118 (29) and most other tested strains (12).
339 Our results indicate that this is due, at least in part, to sodium chloride causing the
340 transcriptional repression of the pilus genes (Fig. 3C).

341 Increases in transcript levels is a hallmark of exposure of *A. baumannii* to $CaCl_2$ and $MgCl_2$
342 alike (Fig. 3A). The transcriptional response is surprinsingly specific and coordinated,
343 inducing all of the type IV pilus genes operons (*pilMONPQ*, *pilA*, f*imU-pilVWXY1-pilE1-*
344 *pilE2*, *pilGHIL-chpA*, *pilBCD*, *pilRS*) but also transformation-specific genes such as *yraN*,
345 *dprA* or *comEA*. This suggests that sensing of Ca^{2+} and Mg^{2+} triggers the activation of a
346 transcriptional regulator. A possible candidate would have been the chemosensory system
347 Pil-chp, integrating sensing by solute binding protein, yet the known response regulators of
348 the Pil-chp system (PilG, PilH) have no role in gene expression, and most importantly,
349 deletion of *chpA, pilG,* or *pilH* did not influence *pilA* expression (28). Another candidate
350 was the main two-component system of the Type IV pilus system, PilRS, possibly acting
351 through the sensing of Ca^{2+} by the type IV pilus adhesin PilY1. PilS directly senses the

352 decrease in periplasmic PilA levels and auto-phosphorylates itself. Transfers of the
353 phosphate to PilR activates the transcription of *pilA* (28) and, according to work on *P.*
354 *aeruginosa,* also of other Type IV pilus operons (42). Ca^{2+} sensing by PilY1 could have
355 stimulated PilA incorporation into the pilus, depleting periplasmic PilA, thus inducing a type
356 IV pilus regulon. However, in a *pilY1* mutant that cannot sense Ca^{2+} and also cannot
357 assemble PilA into a functional pilus, $CaCl_2$ still induces *pilA* expression, indicating that it
358 acts irrespective of the periplasmic levels of PilA sensed by PilRS (Fig 3E). The molecular
359 sensor that can specifically interact with calcium and magnesium ions produce increased
360 levels of mRNA of Type IV pilus genes remains unknown, and may be distinct from
361 classical two-component system involving a transcriptional regulator. One possibility is that
362 the transcriptional response reflects a post transcriptional mechanism. Indeed, the $CaCl_2$
363 effect on *pilA* transcription appears to be moderate (~3-fold increase in transcript)
364 compared to the phenotypic effect (>1,000-fold increase in transformation rate). A similar
365 situation exists in the growth phase variation of PilA protein expression which seems to
366 exceed the 10-fold variation in its mRNA level (28). This may be the sign of a post-
367 transcriptional regulation in which the increase in mRNA levels is not due to transcription
368 but rather to the mRNAs being actively translated, thereby increase their stability and
369 steady-state levels. This would be reminiscent of the control of expression of the minor
370 pilins and the DNA uptake system proteins (ComEA, ComF, ComEC, ComM) in *L.*
371 *pneumophila*, which are all under the post-transcriptional repression of a multi-target non-
372 coding RNA *(23).* Supporting this hypothesis, a new sRNA regulator named ArpA (for
373 *Acinetobacter* repressor of pilin) was found to target the Shine-Dalgarno sequence and the
374 first 17 codon of *pilA* mRNA, blocking its translation and impacting natural transformation
375 and twitching motility (43). Further work is needed to test whether ArpA, or additional
376 sRNA, can simultaneously target in the other type IV pilus operons, *yraN*, *dprA* and
377 *comEA*. If so, the expression of these sRNA might be modulated by calcium and
378 magnesium ions and growth phase.

379 Interestingly, although $CaCl_2$ and $MgCl_2$ seemed identical in the activation of a
380 transformation regulon, transformation efficiencies are about 10-times higher with $CaCl_2$
381 than with $MgCl_2$. This difference may rely on the calcium-binding loop of the non-pilin
382 adhesin PilY1 (also named PilC1 in *Neisseria gonorrhoeae).* In *P. aeruginosa* the calcium
383 binding site of PilY1 is required for twitching motility (34) and in *N. gonorrhoeae* the PilC1
384 calcium-binding mutant had a partial defect in natural transformation (38). Based on
385 genetic and biochemical evidence, PilY1 is proposed to form a complex with minor pilins
386 PilVWX which also interacts with PilE and FimU, acting as connector with the major pilin

387 PilA (37). A more recent model on the *M. xanthus* pilus, based on cryo-electron
388 tomography and protein interaction networks also supports this macromolecular
389 organization where PilY1 sits atop the minor pilin complex (44). AlphaFold predictions of
390 PilY1 structure with PilX, PilV, PilW, FimU, FimT, PilE1, PilE2 and PilA of *A. baumannii* is
391 consistent with the previously proposed models, with all minor pilins forming a helical
392 bundle linking PilY1 to the major pilin PilA. Notably, PilVWX forms a complex beneath
393 PilY1 while FimU-PilE1E2 contact the major pilin PilA. PilY1 contacts with the minor pilin
394 complex by interacting directly with PilX through its the calcium-binding loop. Supporting
395 this hypothesis, the PilY1-PilX interaction is more energetically stable with Ca^{2+}
396 coordinated in the loop. Mg^{2+} may not be the primary ligand of the PilY1 calcium loop and
397 weakly stabilize the interaction between PilX-and PilY1. In *P. aeruginosa*, it was proposed
398 that the PilY1 C-terminal domain bound to Ca^{2+} inhibits PilT-mediated pilus retraction,
399 while the calcium-free PilY1 does not inhibit PilT and allows pilus retraction to proceed.
400 The higher stability of the PilY1-PilX complex when bound to Ca^{2+} support this hypothesis,
401 with a more stable minor pilin complex preventing disassembly and pilus retraction. The
402 interconversion between Ca^{2+}-bound and Ca^{2+}-free PilY1 was proposed to control the
403 cycles of pilus extension and retraction necessary for twitching motility. This hypothesis
404 could be extended here to natural transformation. If Ca^{2+}-binding causes less frequent
405 disassembly, this will result in overall longer residence time of the DNA receptor FimT at
406 the tip of the Type IV pilus (41), increasing the likelihood that DNA can be bound and
407 imported in the periplasmic space.

408 The induction of natural transformation by $CaCl_2$ described here is fundamentally distinct
409 from the use of $CaCl_2$ to artificially induce competence in *Escherichia coli*. In *E. coli*, high
410 concentrations of $CaCl_2$ (millimolar range) are used to transiently alter membrane
411 permeability, allowing passive entry of plasmid DNA that does not efficiently recombine
412 with the chromosome. In contrast, the data support that Ca^{2+} in *A. baumannii* functions as
413 a biological signal, effective at submillimolar concentrations, specifically inducing the
414 coordinated expression and activity of the natural transformation machinery to take up and
415 recombine extracellular DNA. Calcium ions are abundant in host-associated environments
416 (wounds, body fluids) and on medical surfaces frequently colonized by *A. baumannii*.
417 Whether Ca^{2+} contributes to regulation of natural transformation in these settings remains
418 to be determined. However, Ca^{2+} is also abundant and locally variable in soil and aquatic
419 environments and may represent an ecologically meaningful cue. Yet, the environmental
420 reservoirs of *A. baumannii* remain poorly defined and, as of today, the ecological relevance
421 of calcium ions for this species seems difficult to assess. Future work investigating the

422 natural habitat of this species may benefit from including measurements of calcium ion
423 concentrations.

424 Importantly, independent of its ecological and clinical significance, the addition of $CaCl_2$ to
425 NaCl-free growth medium enables efficient natural transformation of *A. baumannii* in liquid
426 culture. $MgCl_2$, although less effective at stimulating transformation, improves bacterial
427 growth and thereby increases the number of transformants recovered. Based on these
428 observations, we established a robust protocol for natural transformation of *A. baumannii*,
429 which will greatly facilitate genome editing by homologous recombination.

430 Material and Methods

431 **Bacterial strains, construction and growth conditions**

432 Bacterial strains and oligonucleotides used in this study are listed in the supplementary
433 tables S1 and S2, respectively. Genetic modifications were made in strain AB5075 (45) or
434 its ΔAbaR11 derivative, AB5075-T (46) and are listed in Table S2. Genetic modifications
435 were obtained using overlap extension PCR to synthesize a large chimeric DNA fragment
436 bordered by 2-kb fragments homologous to the insertion site and as previously described
437 (46). For strain Δ*pilY* and *pilY1*::D947A, we adapted the multiplex genome editing by
438 natural transformation (MuGENT) developed in *V. cholerae* (47). Briefly, this method relies
439 on the cotransformation of two or more PCR fragments by one transformable cell. One
440 PCR fragment carrying a selectable cassette (*aacC4* for apramycin or *tetC* for tetracycline)
441 that integrates into a neutral genomic locus (*att*Tn*7*), is co-transformed along with PCR
442 fragments carrying the desired mutation flanked by 2-Kb homology arms. The optimal yield
443 was obtained when co-transforming 800 ng of non-selectable fragment with 400 ng of
444 selectable fragment. The construction of the *pilA-sfGFP* fusion to follow *pilA* expression is
445 described in the supplementary information along with a new chromosomal expression
446 platform. Strains were grown either in lysogeny broth (LB) or tryptone medium (5g/L Bacto
447 Tryptone, Gibco). All experiments were performed at 37°C. Agarose soluble extract media
448 (ASE) was prepared by adding 0.2 g of agarose D3 (Euromedex) to 10 ml of tryptone
449 media. This suspension was vortexed for 5 min and subsequently centrifuged to sediment
450 the insoluble agarose particles. The supernatant was collected and filtered using a 0.22
451 µm filter.

452 **Construction of a chromosomal expression platform at the attTn*7* locus**

453 We constructed the plasmid pAC-1 that carries the *sacB_aac4* selection/counter-selection
454 cassette and a strong synthetic promoter (Pst) upstream of a reporter gene (*gfp* amplified
455 from from pASG-1 (9)) using an overlap extension PCR into pJET1.2 following
456 manufacturer instructions (CloneJET PCR cloning Kit, Thermofisher scientific). Strong
457 terminators (5S ribosomal RNA and *filA* terminators) were added to obtain the pAC-2
458 plasmid carrying the T_{5S}-*sacB_aacC4_Pst-gfp*-T_{filA} cassette. Chromosomal platforms were
459 constructed in a two-step manner using transformation of overlap extension PCR
460 fragments as described previously (46). First, the T_{5S}-*sacB_aacC4_Pst-gfp*-T_{filA} cassette
461 was inserted in the attTn7 locus by transformation of large chimeric DNA fragment carrying
462 the T_{5S}-*sacB_aacC4_Pst-gfp*-T_{filA} cassette flanked by 2 kb fragments that are homologous
463 to the attTn7 insertion site. The resulting strain was then transformed with a chimeric PCR
464 product carrying a fragment encompassing pilA promoter region and coding sequence and
465 recombinants to replace the *sacB_aacC4*_Pst sequence. Transformants were counter-
466 selected on minimal medium (M63) with 10% sucrose.

467 **Natural transformation conditions for strain constructions**

468 Strains were grown overnight in tryptone medium, followed by dilution in tryptone medium
469 supplemented with $CaCl_2$ (0.68 mM) to obtain a final OD of 0.01. One hundred µl of culture
470 were transferred to a 96-well plate along with 200 ng of transforming DNA and grown at 37
471 °C for a minimum of 7 hours, followed by plating on solid selective media (LB agar plates
472 supplemented with apramycin, 50 µg/L or tetracycline 5 µg/L).

473 **Populational and single cell expression of *pilA*::*gfp***

474 Strains were grown for 16h in tryptone media and diluted to obtain a final optical density
475 (OD_{600}; optical path 1 cm) of 0.01 in the different media tested. Cell density in cultures in
476 96-well plates (Abs_{600}) and fluorescence were monitored every 10 minutes over 8 hours of
477 growth on a Tecan Infinite 200 Pro. The raw fluorescence data was smoothed using a 3-
478 point moving average window and subsequently blank corrected using non-fluorescent
479 wild type cells as control. OD_{600} values were similarly corrected. Expression was calculated
480 by taking the derivative of fluorescence relative to cell density at each time point
481 ($dGFP/dT/Abs_{600}$).

482 Single cell expression was obtained by fluorescence microscopy of cultures at OD_{600} of
483 0.01 (as for populational analysis above) grown for 3 hours in tryptone medium with or
484 without $CaCl_2$ (1 mM). Culture were placed on agar pad on glass slides and imaged with a
485 oil-immersion 60X objective with a EVOS M7000 microscope (Thermofisher Scientific)
486 under phase constrast and under LED illumination for detecting GFP (482/25 nm
487 Excitation; 524/24 nm Emission). Bacterial cells were segmented with Omnipose Cellpose
488 (v4.08) (48) and fluorescence signal was quantified with MicrobeJ (v5.10n) (49).

489 **Gene Expression Analysis and Expression Profiling by RNA-Seq**

490 Pellets from bacterial cultures in various media were stabilized and lysed as previously
491 described using the RNAsnap method (50), followed by RNA extraction as previously
492 described (23, 51). These samples were subsequently treated with DNase I and purified.
493 Ribosomal-depleted RNA were used to construct strand-specific (ASE condition) or
494 unstranded ($CaCl_2$, $MgCl_2$ conditions) libraries, which were sequenced on a Novaseq
495 instrument (Illumina) (GENEWIZ Germany GmbH). Raw read processing and differential
496 expression analyses were carried out using the Curare pipeline (52), using fastp for read
497 trimming, Bowtie2 for alignment to the AB5075-UW reference genome
498 (GCF_031932345.1), and DESeq2 for differential gene expression analysis. Raw reads
499 are available at NCBI under Bioproject Accession number PRJNA1372483.

500 **Transformation assay using luminescence**

501 Transformation assay using luminescence were previously described (10). It is based on
502 the uptake and recombination of the pJET.Ab-pilMNOPQ::nLuc plasmid DNA. As this
503 plasmid is non-replicative in *A. baumannii*, DNA molecules which are internalized undergo
504 a double recombination event allowing the insertion of nanoluc gene in the pilMNOPQ
505 locus and subsequent expression of the NLuc luciferase enzyme. Bacteria from an
506 overnight culture (LB no salt, 10 g/L tryptone, 5 g/L yeast extract) were diluted at an OD_{600}
507 of 0.01 into tryptone medium supplemented with divalent cation when indicated. In a 96-
508 well plate, 100µl were mixed with 250ng of pJET.Ab-pilMNOPQ::nLuc plasmid DNA and
509 incubated overnight (unless indicated otherwise) at 37°C in a static incubator. The optical
510 density of the cell suspension at 600 nm (Abs_{600}) was measured on a Tecan microplate
511 reader. Subsequently, 80 µl of cells were mixed with 20 µl of the mix consisting of Nano-
512 Glo® Luciferase Assay Substrate diluted 1:50 in Luciferase Assay Buffer following the
513 manufacturer instructions (Nano-Glo® Luciferase Assay System, #N1120, Promega).

514 Following incubation at room temperature for 10 minutes, luminescence was measured in
515 a GloMax® Navigator Microplate luminometer (Promega). Relative luminescence units
516 (RLU) were calculated by dividing the luminescence values by the optical density values.

517 **Modeling and free energy analysis of AB5075 type IV pilus initiation complex**

518 The complete structure of the type IV pilus initiation complex comprising the major pilin
519 PilA, the minor pilins (PilX-PilV-PilW-FimU-FimT) and the adhesin PilY1 was modeled
520 using AlphaFold3 server (53). Five independent models were generated and evaluated
521 using the predicted TM-score (pTM), the interface predicted score (iPTM) and ranking
522 confidence metrics provided by Alphafold. The best model with the highest combined
523 confidence values was selected for analysis. Interaction free energy between PilY1-PilX
524 were estimated using the poisson-boltzmann model (PB8) gmx_MMPBSA v1.6 or the
525 generalized born model MMGBSA (GB8) with GROMACS 2023 and the CHARMM36 force
526 field energy with a ionic strength of 150mM as described in (54, 55). The binding free
527 energy ΔG_bind (Kcal/mol) was extracted for each condition and average across replicate
528 minimized model.

529 # Acknowledgements

530 We warmly thank Adrien Ducret for assistance in microscopy image acquisition and
531 analysis.

532 # Funding

533 This work was supported by the French Agence Nationale de la Recherche (ANR), under
534 grant ANR-20-CE12-0004 (TransfoConflict). XC lab is funded by a grant Equipe FRM
535 (Fondation pour la Recherche Médicale) EQU202303016268.

536

References

1. Arnold BJ, Huang I-T, Hanage WP. 2022. Horizontal gene transfer and adaptive evolution in bacteria. Nat Rev Microbiol 20:206–218.

2. Johnston C, Martin B, Fichant G, Polard P, Claverys J-P. 2014. Bacterial transformation: distribution, shared mechanisms and divergent control. Nat Rev Microbiol 12:181–196.

3. WHO updates list of drug-resistant bacteria most threatening to human health. https://www.who.int/news/item/17-05-2024-who-updates-list-of-drug-resistant-bacteria-most-threatening-to-human-health. Retrieved 21 May 2024.

4. Perez F, Stiefel U. 2022. The Impact of Natural Transformation on the Acquisition of Antibiotic Resistance Determinants. mBio 13:e0033622.

5. Mazzamurro F, Touchon M, Charpentier X, Rocha EPC. 2025. Impact of Natural Transformation on the Acquisition of Novel Genes in Bacteria. Mol Biol Evol 42:msaf192.

6. Snitkin ES, Zelazny AM, Montero CI, Stock F, Mijares L, NISC Comparative Sequence Program, Murray PR, Segre JA. 2011. Genome-wide recombination drives diversification of epidemic strains of Acinetobacter baumannii. 33. Proceedings of the National Academy of Sciences 108:13758–13763.

7. Godeux A-S, Svedholm E, Barreto S, Potron A, Venner S, Charpentier X, Laaberki M-H. 2022. Interbacterial Transfer of Carbapenem Resistance and Large Antibiotic Resistance Islands by Natural Transformation in Pathogenic Acinetobacter. mBio 13:e02631-21.

8. Tuffet R, Carvalho G, Godeux A-S, Mazzamurro F, Rocha EPC, Laaberki M-H, Venner S, Charpentier X. 2024. Manipulation of natural transformation by AbaR-type islands promotes fixation of antibiotic resistance in Acinetobacter baumannii. Proc Natl Acad Sci U S A 121:e2409843121.

9. Godeux A-S, Lupo A, Haenni M, Guette-Marquet S, Wilharm G, Laaberki M-H, Charpentier X. 2018. Fluorescence-Based Detection of Natural Transformation in Drug-Resistant Acinetobacter baumannii. Journal of Bacteriology 200:e00181-18.

10. Mazzamurro F, Chirakadavil JB, Durieux I, Poiré L, Plantade J, Ginevra C, Jarraud S, Wilharm G, Charpentier X, P C Rocha E. 2024. Intragenomic conflicts with plasmids and chromosomal mobile genetic elements drive the evolution of natural transformation within species. PLoS Biol 22:e3002814.

11. Vesel N, Iseli C, Guex N, Lemopoulos A, Blokesch M. 2023. DNA modifications impact natural transformation of Acinetobacter baumannii. Nucleic Acids Res 51:5661–5677.

12. Hu Y, He L, Tao X, Meng F, Zhang J. 2019. High DNA Uptake Capacity of International Clone II Acinetobacter baumannii Detected by a Novel Planktonic Natural Transformation Assay. Front Microbiol 10:2165.

13. Dubnau D, Blokesch M. 2019. Mechanisms of DNA Uptake by Naturally Competent Bacteria. Annu Rev Genet 53:217–237.

14. Craig L, Forest KT, Maier B. 2019. Type IV pili: dynamics, biophysics and functional consequences. Nat Rev Microbiol 17:429–440.

15. Nguyen Y, Sugiman-Marangos S, Harvey H, Bell SD, Charlton CL, Junop MS, Burrows LL. 2015. Pseudomonas aeruginosa Minor Pilins Prime Type IVa Pilus Assembly and Promote Surface Display of the PilY1 Adhesin. J Biol Chem 290:601–611.

16. Guo S, Chang Y, Brun YV, Howell PL, Burrows LL, Liu J. 2024. PilY1 regulates the dynamic architecture of the type IV pilus machine in Pseudomonas aeruginosa. Nat Commun 15:9382.

17. Treuner-Lange A, Chang Y-W, Glatter T, Herfurth M, Lindow S, Chreifi G, Jensen GJ, Søgaard-Andersen L. 2020. PilY1 and minor pilins form a complex priming the type IVa pilus in Myxococcus xanthus. Nat Commun 11:5054.

18. Stedman MJM, Deselaers S, Braus SAG, Wang D, Balaguer MG, Gossert AD, Hospenthal MK. 2025. Molecular interplay between ComEC domains allows for selective degradation of the non-translocating strand during natural transformation. Nucleic Acids Res 53:gkaf932.

19. Mortier-Barrière I, Velten M, Dupaigne P, Mirouze N, Piétrement O, McGovern S, Fichant G, Martin B, Noirot P, Le Cam E, Polard P, Claverys J-P. 2007. A key presynaptic role in transformation for a widespread bacterial protein: DprA conveys incoming ssDNA to RecA. Cell 130:824–36.

20. Hardy L, Morales V, Rousseau CJ, Bergé M, Mazzamurro F, Plantade J, Dalia TN, Dalia AB, Rocha EPC, Charpentier X, Polard P. 2026. Two D-loop resolution systems enable natural genetic transformation in bacteria. bioRxiv https://doi.org/10.1101/2024.02.06.579203.

21. Nero TM, Dalia TN, Wang JC-Y, Kysela DT, Bochman ML, Dalia AB. 2018. ComM is a hexameric helicase that promotes branch migration during natural transformation in diverse Gram-negative species. Nucleic Acids Res 46:6099–6111.

22. Dalia AB, Dalia TN. 2019. Spatiotemporal Analysis of DNA Integration during Natural Transformation Reveals a Mode of Nongenetic Inheritance in Bacteria. Cell 179:1499-1511.e10.

23. Attaiech L, Boughammoura A, Brochier-Armanet C, Allatif O, Peillard-Fiorente F, Edwards RA, Omar AR, MacMillan AM, Glover M, Charpentier X. 2016. Silencing of natural transformation by an RNA chaperone and a multitarget small RNA. Proc Natl Acad Sci USA 113:8813–8818.

24. Meibom KL, Blokesch M, Dolganov NA, Wu C-Y, Schoolnik GK. 2005. Chitin induces natural competence in Vibrio cholerae. Science 310:1824–1827.

25. Taton A, Erikson C, Yang Y, Rubin BE, Rifkin SA, Golden JW, Golden SS. 2020. The circadian clock and darkness control natural competence in cyanobacteria. Nat Commun 11:1688.

26. Wilharm G, Piesker J, Laue M, Skiebe E. 2013. DNA uptake by the nosocomial pathogen Acinetobacter baumannii occurs during movement along wet surfaces. J Bacteriol 195:4146–4153.

27. Harding CM, Tracy EN, Carruthers MD, Rather PN, Actis LA, Munson RS. 2013. Acinetobacter baumannii Strain M2 Produces Type IV Pili Which Play a Role in Natural Transformation and Twitching Motility but Not Surface-Associated Motility. mBio 4.

28. Vesel N, Blokesch M. 2021. Pilus Production in Acinetobacter baumannii Is Growth Phase Dependent and Essential for Natural Transformation. Journal of Bacteriology 203.

29. Domingues S, Rosário N, Cândido Â, Neto D, Nielsen KM, Da Silva GJ. 2019. Competence for Natural Transformation Is Common among Clinical Strains of Resistant Acinetobacter spp. Microorganisms 7:30.

30. Yu Y, Mahdi R, Al-Hilfy Leon A, Vo N, Lofgren R, Mutabazi JL, Piepenbrink KH. 2025. Variation in type IV pilus stability modulates DNA uptake and biofilm formation. J Biol Chem 301:110787.

31. Traglia GM, Quinn B, Schramm STJ, Soler-Bistue A, Ramirez MS. 2016. Serum Albumin and Ca2+ Are Natural Competence Inducers in the Human Pathogen Acinetobacter baumannii. 8. Antimicrob Agents Chemother 60:4920–4929.

32. Yarrington KD, Limoli DH. 2025. The type IV pilus steering committee: how Pil-Chp controls directional motility. Journal of Bacteriology 207:e00396-24.

33. Kilmury SLN, Burrows LL. 2016. Type IV pilins regulate their own expression via direct intramembrane interactions with the sensor kinase PilS. Proceedings of the National Academy of Sciences 113:6017–6022.

34. Orans J, Johnson MDL, Coggan KA, Sperlazza JR, Heiniger RW, Wolfgang MC, Redinbo MR. 2010. Crystal structure analysis reveals Pseudomonas PilY1 as an essential calcium-dependent regulator of bacterial surface motility. Proc Natl Acad Sci U S A 107:1065–1070.

35. Herfurth M, Treuner-Lange A, Glatter T, Wittmaack N, Hoiczyk E, Pierik AJ, Søgaard-Andersen L. 2022. A noncanonical cytochrome c stimulates calcium binding by PilY1 for type IVa pili formation. Proceedings of the National Academy of Sciences 119:e2115061119.

36. Ellison CK, Dalia TN, Klancher CA, Shaevitz JW, Gitai Z, Dalia AB. 2021. Acinetobacter baylyi regulates type IV pilus synthesis by employing two extension motors and a motor protein inhibitor. Nat Commun 12:3744.

37. Nguyen Y, Sugiman-Marangos S, Harvey H, Bell SD, Charlton CL, Junop MS, Burrows LL. 2015. Pseudomonas aeruginosa Minor Pilins Prime Type IVa Pilus Assembly and Promote Surface Display of the PilY1 Adhesin. J Biol Chem 290:601–611.

38. Cheng Y, Johnson MDL, Burillo-Kirch C, Mocny JC, Anderson JE, Garrett CK, Redinbo MR, Thomas CE. 2013. Mutation of the Conserved Calcium-Binding Motif in Neisseria gonorrhoeae PilC1 Impacts Adhesion but Not Piliation. Infect Immun 81:4280–4289.

39. Ellison CK, Kan J, Dillard RS, Kysela DT, Ducret A, Berne C, Hampton CM, Ke Z, Wright ER, Biais N, Dalia AB, Brun YV. 2017. Obstruction of pilus retraction stimulates bacterial surface sensing. Science 358:535–538.

40. Siryaporn A, Kuchma SL, O'Toole GA, Gitai Z. 2014. Surface attachment induces Pseudomonas aeruginosa virulence. Proceedings of the National Academy of Sciences 111:16860–16865.

41. Ellison TJ, Ellison CK. 2025. Improved DNA binding to a type IV minor pilin increases natural transformation. Nucleic Acids Res 53:gkaf467.

42. Kilmury SLN, Burrows LL. 2018. The Pseudomonas aeruginosa PilSR Two-Component System Regulates Both Twitching and Swimming Motilities. mBio 9:e01310-18.

43. Hamrock FJ, Guest T, Daum MN, Connell O, Ershova AS, Hokamp K, Fleming AB, Gebhardt MJ, Westermann AJ, Kröger C. 2025. DNA uptake and twitching motility are controlled by the small RNA Arp through repression of pilin translation in Acinetobacter baumannii. bioRxiv 2025.07.19.665661.

44. Treuner-Lange A, Chang Y-W, Glatter T, Herfurth M, Lindow S, Chreifi G, Jensen GJ, Søgaard-Andersen L. 2020. PilY1 and minor pilins form a complex priming the type IVa pilus in Myxococcus xanthus. Nat Commun 11:5054.

45. Jacobs AC, Thompson MG, Black CC, Kessler JL, Clark LP, McQueary CN, Gancz HY, Corey BW, Moon JK, Si Y, Owen MT, Hallock JD, Kwak YI, Summers A, Li CZ, Rasko DA, Penwell WF, Honnold CL, Wise MC, Waterman PE, Lesho EP, Stewart RL, Actis LA, Palys TJ, Craft DW, Zurawski DV. 2014. AB5075, a Highly Virulent Isolate of Acinetobacter baumannii, as a Model Strain for the Evaluation of Pathogenesis and Antimicrobial Treatments. MBio 5:e01076-01014.

46. Godeux A-S, Svedholm E, Lupo A, Haenni M, Venner S, Laaberki M-H, Charpentier X. 2020. Scarless Removal of Large Resistance Island AbaR Results in Antibiotic Susceptibility and Increased Natural Transformability in Acinetobacter baumannii. Antimicrob Agents Chemother 64.

47. Dalia AB, McDonough E, Camilli A. 2014. Multiplex genome editing by natural transformation. Proceedings of the National Academy of Sciences 111:8937–8942.

48. Cutler KJ, Stringer C, Lo TW, Rappez L, Stroustrup N, Brook Peterson S, Wiggins PA, Mougous JD. 2022. Omnipose: a high-precision morphology-independent solution for bacterial cell segmentation. Nat Methods 19:1438–1448.

49. Ducret A, Quardokus EM, Brun YV. 2016. MicrobeJ, a tool for high throughput bacterial cell detection and quantitative analysis. Nat Microbiol 1:16077.

50. Stead MB, Agrawal A, Bowden KE, Nasir R, Mohanty BK, Meagher RB, Kushner SR. 2012. RNAsnap™: a rapid, quantitative and inexpensive, method for isolating total RNA from bacteria. Nucleic Acids Res 40:e156.

51. Durieux I, Ginevra C, Attaiech L, Picq K, Juan P-A, Jarraud S, Charpentier X. 2019. Diverse conjugative elements silence natural transformation in Legionella species. PNAS 116:18613–18618.

52. Blumenkamp P, Pfister M, Diedrich S, Brinkrolf K, Jaenicke S, Goesmann A. 2024. Curare and GenExVis: a versatile toolkit for analyzing and visualizing RNA-Seq data. BMC Bioinformatics 25:138.

53. Abramson J, Adler J, Dunger J, Evans R, Green T, Pritzel A, Ronneberger O, Willmore L, Ballard AJ, Bambrick J, Bodenstein SW, Evans DA, Hung C-C, O'Neill M, Reiman D, Tunyasuvunakool K, Wu Z, Žemgulytė A, Arvaniti E, Beattie C, Bertolli O, Bridgland A, Cherepanov A, Congreve M, Cowen-Rivers AI, Cowie A, Figurnov M, Fuchs FB, Gladman H, Jain R, Khan YA, Low CMR, Perlin K, Potapenko A, Savy P, Singh S, Stecula A, Thillaisundaram A, Tong C, Yakneen S, Zhong ED, Zielinski M, Žídek A, Bapst V, Kohli P, Jaderberg M, Hassabis D, Jumper JM. 2024. Accurate structure prediction of biomolecular interactions with AlphaFold 3. Nature 630:493–500.

54. Hou T, Wang J, Li Y, Wang W. 2011. Assessing the performance of the MM/PBSA and MM/GBSA methods. 1. The accuracy of binding free energy calculations based on molecular dynamics simulations. J Chem Inf Model 51:69–82.

55. Wang S, Sun X, Cui W, Yuan S. 2022. MM/PB(GB)SA benchmarks on soluble proteins and membrane proteins. Front Pharmacol 13:1018351.